

Investigation For Output Torque Of A Low Pressure Water Hydraulic Planetary Gear Motor

Shigeru OSHIMA, Takuya HIRANAO

Abstract: This study concerns a Planetary Gear Motor which can be driven by low pressure as same as civil tap water pressure. Low pressure water hydraulic system has advantages such as low cost, safety and easy usage as well as no risk to pollute the environment if leakage happens. The purpose of this paper is to introduce the structure of the Low Pressure Water hydraulic Planetary Gear Motor (LPW-PGM) and to explain the supposed mechanism of output torque generation and the method to calculate the theoretical output torque. The theoretically calculated output torque is compared with the measured under the condition of very low constant rotational speed. As a result, it is found that there is a difference between the calculated and measured results, and the major of difference is caused by the friction at the meshing parts on the teeth of the stator, rotor and planetary gears. The experimental result shows that a surface treatment on the planetary gears with solid lubricant film which contains Graphite makes the output torque efficiency increase about 15%. In addition, the planetary gears made of PEEK and brass are also tested.

Key words: Water Hydraulics, Low Pressure, Planetary Gear Motor, Output Torque

1 Introduction

Water hydraulic system which uses tap water as a pressure medium has no risk to pollute the environment if leakage happens. It has been known, therefore, as an environmental friendly new fluid power drive system since the late of 20th century. It has many advantages; clean, non-

toxic, non-flammable, low pressure loss, and so on¹⁾. It is also a big advantage that the pressure medium is easily obtained and drained. It leads to decreasing of management cost, too.

The water hydraulic systems are considered to have many possible applications in low pressure driving field as well as in middle and high pressure driving. The low pressure leads to the low cost of components, and the easy operation and safety driving of the systems. Studies on the low pressure water hydraulic systems have been carried out to aim to get the low price in compatible to pneumatic systems while high power density and good controllability are compatible to oil hydraulic systems^{2), 3)}.

Water hydraulic systems have been applied in industries of food

processing, beverage bottling and packaging, semiconductor and paper manufacturing, etc. There are also possible applications in welfare equipments, universal house equipments, leisure and amusements park equipments and others⁴⁾. For the many of those applications, the low pressure water hydraulic systems are available. Some of them can be driven directly by the pressure from the civil tap water network or the water supply network for the industries. Otherwise, centrifugal pumps may be often installed as pressure sources. Anyway, it is relatively easy to get the pressure source for the low pressure water hydraulic systems.

The goal of this study is to develop a Low Pressure Water hydraulic Planetary Gera Motor (LPW-PGM), which can be driven by low pressure as same as civil tap water pressure. The planetary gear motor has been

Professor Shigeru Oshima, Numazu National College of Technology, Department of Control & Computer Engineering 3600 Okoa, Numazu, Shizuoka, 410-8501 Japan
Takuya Hirano, Suntory Liquors Limited, Osaka Plant Blend Group, 3-2-30 Kaigandori, Minato-ku, Osaka City, Osaka, 552-0022 Japan

developed originally in Holland as a low-speed high-torque hydraulic motor. The basic principle and theory for its geometry have been reported in detail in the reference material⁵⁾. Based on the theory in the report, we made a prototype to be available for the low pressure water hydraulic systems. The purpose of this paper is to introduce the structure of LPW-PGM and to explain the supposed mechanism of output torque generation and the method to calculate the theoretical output torque. The theoretically calculated output torque is compared with the measured under the condition of very low constant rotational speed. As a result, it is found that there is a difference between the calculated and measured results, and the major of difference is caused by the friction at the meshing parts on the teeth of the stator, rotor and planetary gears. The experimental result shows that a surface treatment on the planetary gears with solid lubricant film which contains Graphite makes the output torque efficiency increase about 15%. In addition, the planetary gears made of PEEK and brass are also tested.

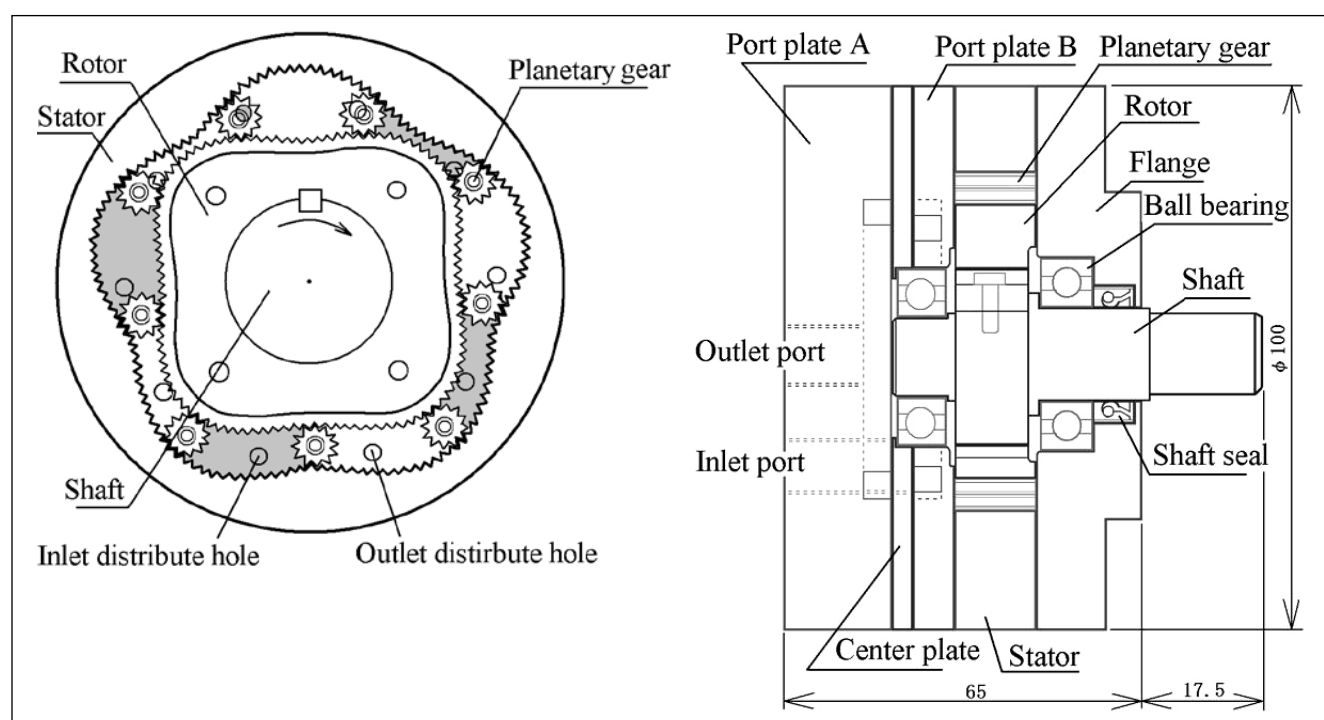
■ 2 Structure and mechanism of torque generation

2.1 Structure and dimensions

The main part of the LPW-PGM consists of a stator, a rotor, nine planetary gears, port plates A, B and a flange as shown in Figure 1. In our prototype, the inside of the stator is formed by a curve with 5 lobes and the outside of the rotor is formed by a curve with 4 lobes. The geometry (shape and size) of the pitch curves of them and the radius of the planetary gear's pitch circle have a tight connection. They are all determined by numerical calculation of the equations derived based on the theorem of friction wheel model⁵⁾. The curved surfaces of the stator and the rotor have teeth which mesh with the planetary gears' teeth. Nine displacement chambers are formed, which are enclosed by the stator, rotor, planetary gears, port plate B and flange. The each chamber's volume varies periodically when the rotor rotates.

The port plate A has an outlet port and five outlet distribute holes

which are all connected with a pentagon groove and the port plate B has an inlet port and five inlet distribute holes which are all connected with a pentagon groove such as shown in Figure 2. The inlet port is also drilled through the port plate A to connect the inlet port on the port plate B, and the five outlet distribute holes are also drilled through the port plate B at the same place of each the outlet distribute hole on the port plate A. The inlet distribute holes and the outlet distribute holes are located alternately on the inside surface of the port plate B and open to the displacement chambers as shown in Figure 1. Each displacement chamber connects alternately to an inlet distribute hole and an outlet distribute hole when the rotor rotates. The volume of each displacement chamber increases when connecting to the inlet distribute hole and decreases when connecting to the outlet distribute hole. Water is supplied to the inlet port and the water discharged from the chamber is exhausted through the outlet distribute holes to the outlet port which is connected to a return line.



(a) Structure of main part

(b) Cross sectional side view

Figure 1. Structure of the LPW-PGM

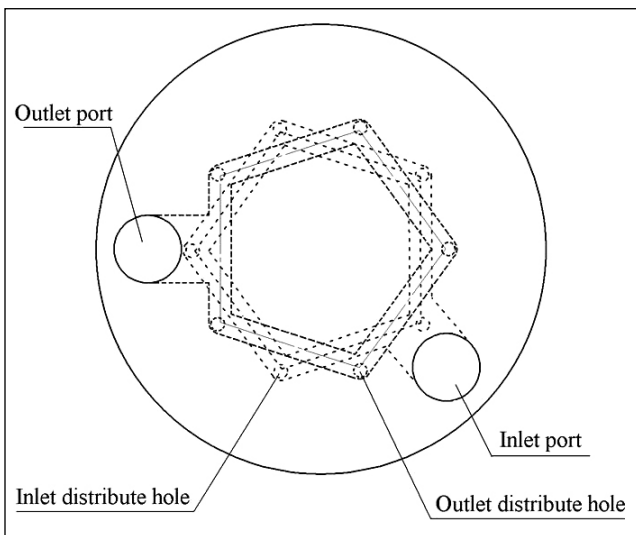


Figure 2. Location of Inlet and Outlet distribute holes on the port plates A and B

In the theoretical analysis, the connection of the rotor, stator and planetary gears are treated as a friction wheel model as shown in Figure 3. The tooth profile has been removed from the pitch curves and pitch circles of them. The pitch circle of the planetary gear is always in contact with the pitch curves of the rotor and stator. The stator is considered fixed in space, the rotor rotates around its axis "O", and the planetary gears roll on the pitch curves of the rotor and the stator with no slip when the rotor rotates.

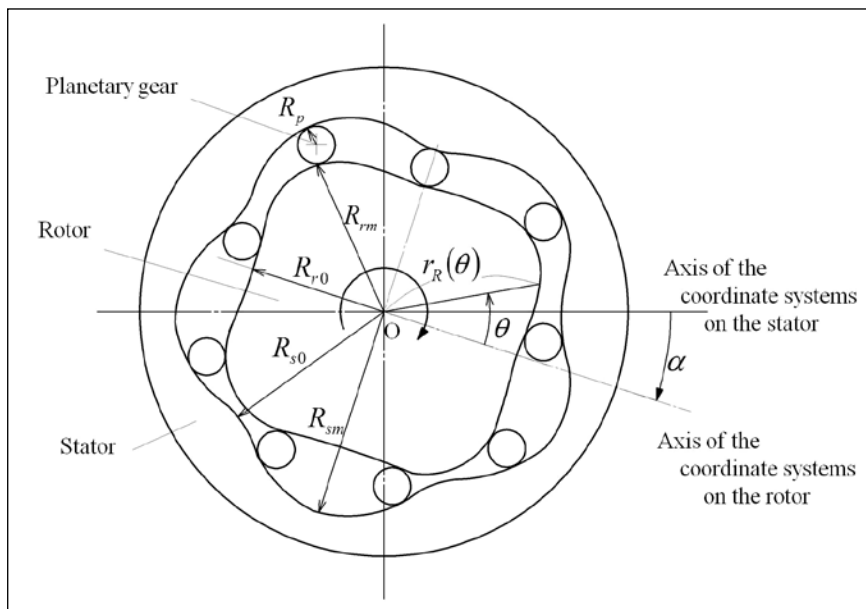
The rotor's pitch curve of our prototype is formed by a cosine curve by Equation (1), of which the minimum radius R_{r0} , the maximum radius R_m and the number of lobes N_{rRL} are initially determined by a designer.

$$r_r(\theta) = R_{r0} + \frac{R_m - R_{r0}}{2} \{1 + \cos(N_{rRL} \cdot \theta + \pi)\} \quad (1)$$

The stator's pitch curve geometry is determined as the trace of the contact point of the planetary gear and the stator. There is only one possible radius of the planetary gear for a given number of stator lobes N_{rSL} when the rotor's pitch curve geometry is determined. The equations to solve the problems to find the planetary gear's radius and the stator's pitch curve geometry are presented in the report⁵⁾. Authors made a computer program to calculate the equations numerically to get the geometries of

them. The practical dimensions of the main parts of the prototype are shown in Figure 3. In practice, the rotor has 104 teeth, the stator has 130 teeth on their pitch curves by numerical integration is 36.6 cm³/rev. The rated output power of

shows the mechanism of torque generation at one of displacement chambers connected to the inlet distribute holes. The drawing of (a) shows the generation of torque by the pressure acts on the rotor surface and (b) shows that on the planetary gears. Note that there is a distance l_2 between the center of the rotor and the force acting line of F_r in (a), and r_1 is larger than r_2 in (b). It causes the torque in clockwise. The same condition appears at the all displacement chambers when they connect to the inlet distribute holes. As the planetary gears revolve with the rotation of the rotor, the displacement chambers move and switch the connection to the inlet



$N_{rRL} = 4$, $N_{rSL} = 5$, $R_{r0} = 22.55$ mm, $R_{rm} = 27.52$ mm, $R_{s0} = 28.54$ mm, $R_{sm} = 33.51$ mm, $R_p = 3.00$ mm, $W_p = 15.00$ mm

Figure 3. Friction wheel model for theoretical analysis

the prototype is 15 Nm/s, the output torque is 0.75 Nm and the rotational speed is 200 rpm when it is driven at 0.25 MPa and 8.5 L/min⁶⁾.

2.2 Mechanism of torque generation

In the displacement chambers which connect to the inlet distribute holes, the shadowed chambers in Figure 1, the pressure acts on the rotor surface and the planetary gears generates the torque in clockwise. Figure 4

and outlet distribute holes by turns. The rotation of the rotor, therefore, continues while pressurized water is supplied to the inlet port.

3 Calculation of Theoretical Output Torque

3.1 Equations for calculation

Referring Figure 4, the equations to calculate the theoretical output torque are presented as follows. The

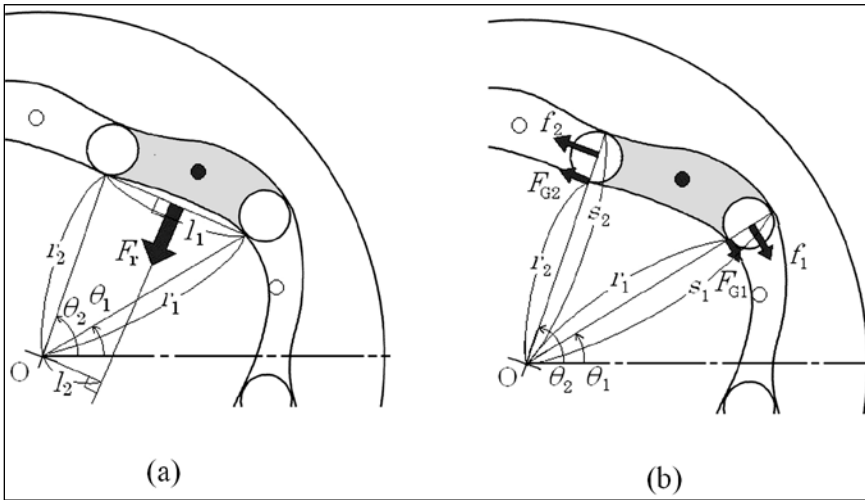


Figure 4. Mechanism of torque generation

force F_r shown in (a) is presented by Eq. (2),

$$F_r = l_1 \cdot W_p \cdot P_c \quad (2)$$

here the distance l_1 is by Eq.(3).

$$l_1 = \sqrt{r_1^2 + r_2^2 - 2r_1r_2 \cos(\theta_2 - \theta_1)} \quad (3)$$

The positions of the contact points (r_1, θ_1) and (r_2, θ_2) are obtained for each given rotational angle α by numerical calculation with the computer program made by us based on the theorem of friction wheel model ⁵⁾. Then, the torque T_r generated by F_r at each α is calculated by Eq. (4).

$$T_r = F_r \cdot l_2 \quad (4)$$

Here, the length of the distance l_2 is calculated geometrically assuming that the force acting line of F_r is the perpendicular bisector of the line shown with the length l_1 .

The forces f_1 and f_2 act on the planetary gears shown in (b) of Figure 4 are presented by Eq. (5) and Eq. (6).

$$f_1 = (s_1 - r_1) \cdot W_p \cdot P_c \quad (5)$$

$$f_2 = (s_2 - r_2) \cdot W_p \cdot P_c \quad (6)$$

The contact point of a planetary gear and the stator is on the same line which is through the contact point of the planetary gear and the rotor. The polar coordinates positions of the contact points (s_1, θ_1) and (s_2, θ_2) are calculated numeri-

cally by the computer program made by us as same as the contact points (r_1, θ_1) and (r_2, θ_2) . Since the tangential forces F_{G1} and F_{G2} which act on the surface of the rotor at the contact points are $f_1/2$ and $f_2/2$ respectively, the torque T_G is presented by Eq. (7).

$$T_G = F_{G1} \cdot r_1 - F_{G2} \cdot r_2 \quad (7)$$

The theoretical output torque T_{th} , which is ideal torque without any torque loss, is given as the sum of T_r and T_G , which are generated at the nine displacement chambers, by Eq. (8).

$$T_{th} = \sum_{i=1}^9 (T_r + T_G)_i \quad (8)$$

3.2 Calculation and the Result

The theoretical output torque T_{th} is calculated numerically at each the rotational angle α with a step of 0.1 degree for the one rotation of the rotor. The polar coordinates positions of the contact points of the

nine planetary gears' pitch circles and the pitch curves of the rotor and the stator are calculated numerically at the each rotational angle α . Then the theoretical output torque is calculated by the equations presented above. In the calculation, the pressure in the displacement chamber is assumed that it is equal to the supply pressure P_s when the inlet distribute hole opens to the chamber as shown in Figure 5 (a), it is equal to the half of the supply pressure when the both of the inlet and outlet distribute holes are covered by the planetary gears as shown in (b), and it is equal to zero when the outlet distribute hole opens to the chamber as shown in (c).

A result of the calculation of the theoretical output torque T_{th} when the supply pressure is 0.25 MPa is shown in Figure 6. It shows also the waves of the theoretical torque generated at the each displacement chamber for the all of the nine chambers. An each displacement chamber generates the torque with 2 and 2/9 times during the one rotation of the rotor as shown in Figure 6. Four or five displacement chambers simultaneously generate the torque, and the sum of them is the value of T_{th} at each moment. It is found that there are periodical twenty ripples on T_{th} for the one rotation of the rotor. The average value of T_{th} is 1.43 Nm, and it is very close to the theoretical torque 1.46 Nm calculated by Eq. (9).

$$T_{th} = \frac{\Delta P \cdot V_{th}}{2\pi} \quad (9)$$

It is found that negative torque appears slightly on the waves of the theoretical torque generated at each a displacement chamber. The reason is considered as the follow-

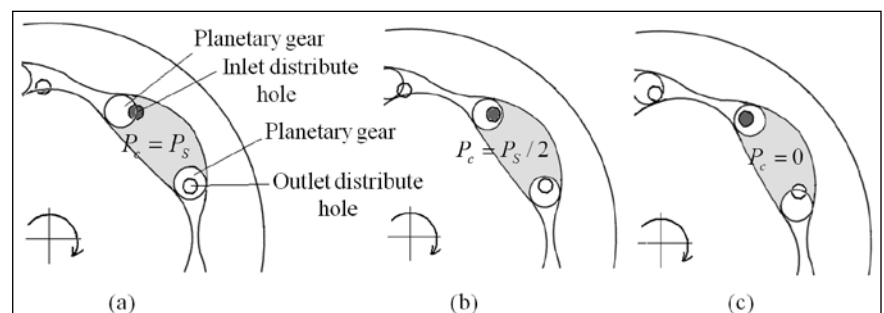


Figure 5. Assumption for the pressure in the displacement chamber

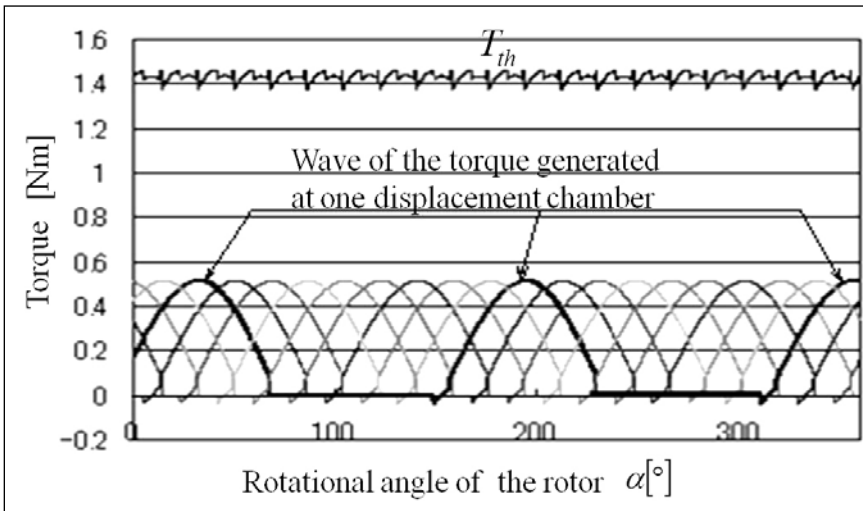


Figure 6. A result of calculation of the theoretical output torque (at $P_s=0.25$ MPa)

ing. When a displacement chamber switches the connection from with the outlet distribute hole to with the inlet distribute hole, the both of the inlet and outlet distribute holes are covered by the planetary gears for a moment. In our calculation, under such the condition, the pressure in the chamber is assumed to be equal to the half of the supply pressure. From the detail consideration on the geometrical condition in Figure 4, it is found that the state of $l_2 < 0$ and $r_1 < r_2$ is still there for a moment when the both of the inlet and outlet distribute holes are covered by the planetary gears. It results in the generation of the negative torque.

■ 4 Experiment

The output torque of a prototype of the LPW-PGM is measured in order to compare with the theoretical calculation result. The measurement is carried out under the condition of very low constant rotational speeds using the experimental setup shown in Figure 7. Why the condition of the low rotational speed is better for this measurement, because the pressure drop on the passages inside the motor has a pretty large effect on the output torque because the supply pressure is very low. Therefore, the less flow rate is the better for this measurement.

Water from a piston pump is set at a given pressure by a relief valve and a throttle valve, and supplied

to the LPW-PGM. Its shaft tends to rotate but it cannot rotate freely because it is connected to the shaft of the torque detector of which shaft is connected to the output shaft of the worm gear decelerator with reduction ratio 50. The shaft of the LPW-PGM rotates only at a constant speed which is regulated by the worm gear decelerator and AC servo motor. The rotational speed is set by frequency of input signal to the driver unit of AC servo motor. The output torque of the LPW-PGM is detected

by a torque detector and acquired by PC corresponding to each pulse signal from a rotary encoder which makes 900 pulses per one rotation of the shaft of the LPW-PGM. The data acquisition starts by a trigger signal from a limit switch. The pressures P_s and P_{out} are measured with Bourdon pressure gauges, and the flow rate with the turbine flow meter of which range is 0.75 to 7.5 L/min. The output torque is measured with a torque detector and a data processing unit which has analog output function. The capacity of the torque detector is 2.0 Nm.

The main parts; stator, rotor, planetary gears, shaft, flange and port plate B of the original prototype are made of stainless steel. Only the port plate A and the center plate are made of aluminum. The flange and the port plate B have treatment with DLC on their surfaces to reduce the friction between their surfaces and the contacting faces of rotor and planetary gears.

Figure 8 shows the measured output torque of the original prototype when the rotational speed is 1 rpm and the supply pressure

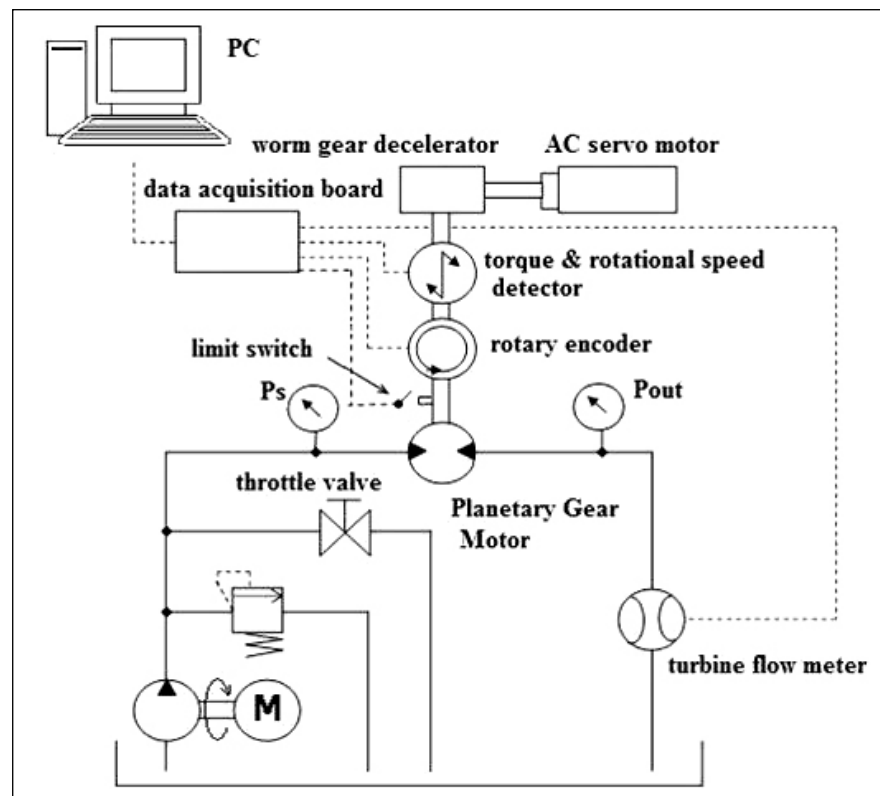


Figure 7. Experimental setup

is 0.25 MPa. The average value of the output torque is 1.11 Nm and there are considerable large fluctuations of which the peak to peak value is about 0.59 Nm in maximum. The measurements were also carried out at the different rotational speeds; 0.1, 2 and 3 rpm, and their results were almost the same as the result of Figure 8. The average values and the peak to peak values of the fluctuations in the measured output torque of the original prototype are shown in Table 1. The ratio of the average value of the four average values to the theoretical re-

sult's average value 1.43 Nm is 0.74. The material of rotor and stator is the same stainless steel of SAE grade 304, and the planetary gear is 316 in the original prototype. It is considered that there is considerable large friction on the meshing teeth of the rotor, the stator and the planetary gears.

In order to reduce the friction on the meshing teeth, the surface of the planetary gears are put a treatment with solid lubricant film which contains Graphite. The surface treatment on the planetary gears shows a good effect. Figure 9 shows the

measured output torque of the prototype of which the planetary gears are replaced with the planetary gears put the treatment with solid lubricant film. The average value of the output torque increases to 1.28 Nm and the maximum peak to peak value of the fluctuation decreases to 0.23 Nm. The average values and the maximum peak to peak values of the fluctuations under the several different rotational speeds and supply pressures are shown in Table 2. The ratio of the average value of the four average values when $P_s=0.25$ MPa to the theoretical average value is increased to 0.89. From these results, it is found that the friction on the meshing teeth has considerably a large effect on the torque efficiency.

Concerning the effect of the surface treatment with solid lubricant film which contains Graphite, it is reported that it has been very effective to improve the fretting fatigue strength of aluminum alloy because the solid lubricant film has low friction coefficient and prevents the test specimen surface from metal-to-metal contact for a long term ⁷⁾.

An engineering plastic PEEK is expected to be effective to reduce the friction on the meshing teeth. The

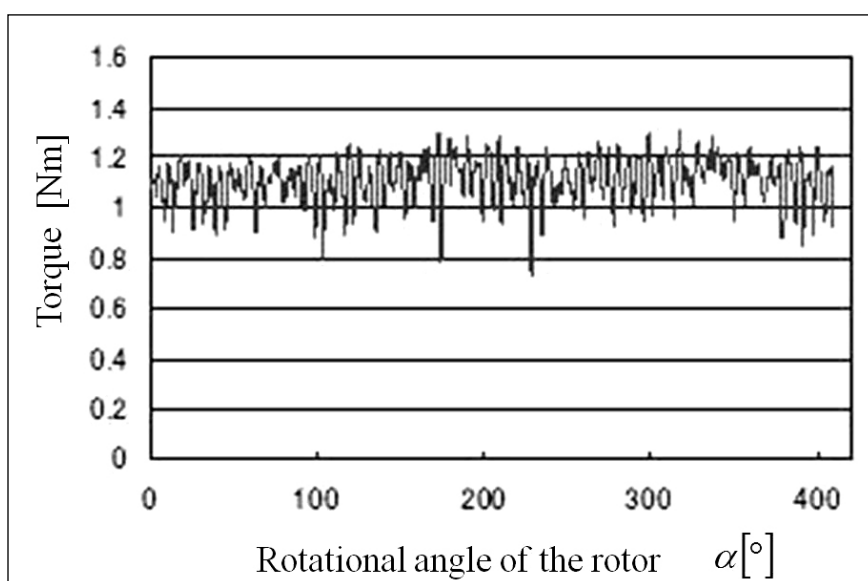


Figure 8. Measured output torque of the original prototype (at 1 rpm and $P_s=0.25$ MPa)

Table 1. Average values and the maximum peak to peak values of the fluctuations in the measured output torque of the original prototype

Rotational speed (rpm)	Output torque	$P_s = 0.2$ MPa	$P_s = 0.25$ MPa	$P_s = 0.3$ MPa
0.1	Average value	–	1.08 Nm	–
	Max. value of the peak to peak	–	0.59 Nm	–
1	Average value	0.87 Nm	1.11 Nm	1.26 Nm
	Max. value of the peak to peak	0.42 Nm	0.59 Nm	0.70 Nm
2	Average value	–	1.02 Nm	–
	Max. value of the peak to peak	–	0.72 Nm	–
3	Average value	–	1.03 Nm	–
	Max. value of the peak to peak	–	0.55 Nm	–

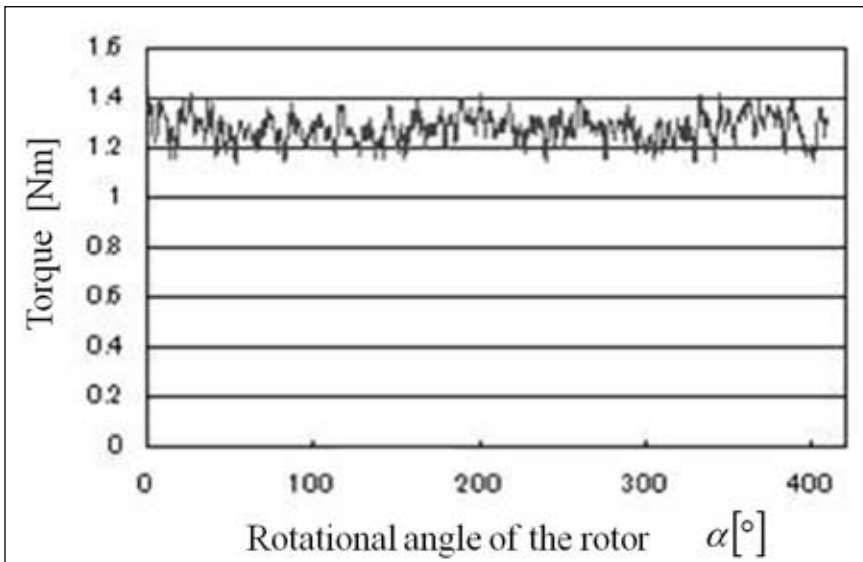


Figure 9. Measured output torque when using the planetary gears with surface treatment of solid lubricant film (at 1 rpm and $P_s=0.25$ MPa)

the surface treatment with solid lubricant film. There is still remained the difference of 0.15 Nm between the average values of the theoretical and the experimental results. Since the theoretical result contains no torque loss, the difference is due to the torque losses generated at several parts inside the LPW-PGM. The torque losses by the friction on the meshing teeth still may be remained, and also there may be the torque losses induced by friction at the other sliding parts; among the inside faces of the flange and the port plate B and the side faces of the rotor and the planetary gears, at the bearings and the shaft seal. The reduction of those torque losses will be expected to get the higher torque efficiency.

Table 2. Average values and the maximum peak to peak values of the fluctuations in the output torque when using the planetary gears with surface treatment of solid lubricant film

Rotational speed (rpm)	Output torque	$P_s = 0.2$ MPa	$P_s = 0.25$ MPa	$P_s = 0.3$ MPa
0.1	Average value	0.98 Nm	1.26 Nm	1.53 Nm
	Max. value of the peak to peak	0.30 Nm	0.27 Nm	0.39 Nm
1	Average value	0.99 Nm	1.28 Nm	1.55 Nm
	Max. value of the peak to peak	0.28 Nm	0.23 Nm	0.38 Nm
2	Average value	0.99 Nm	1.28 Nm	1.53 Nm
	Max. value of the peak to peak	0.31 Nm	0.28 Nm	0.36 Nm
3	Average value	1.00 Nm	1.25 Nm	1.53 Nm
	Max. value of the peak to peak	0.32 Nm	0.27 Nm	0.33 Nm

planetary gears made of PEEK and brass are also tested in the same conditions. The average values gained at 1 rpm are shown in Table 3. It is found that the planetary gear made with PEEK gives pretty good improvement in output torque while the brass dose not so good.

Table 3. Average values of measured output torque when using the planetary gears made of PEEK and Brass (at 1 rpm)

Planetary Gear	$P_s = 0.2$ MPa	$P_s = 0.25$ MPa	$P_s = 0.3$ MPa
PEEK	1.06 Nm	1.34 Nm	1.60 Nm
Brass	0.91 Nm	1.16 Nm	1.38 Nm

■ 5 Comparison of Theoretical and Experimental Results

The calculated results of the output torque shown in Figure 6 and Figure

9 are shown comparing in Figure 10. The ratio of the average value of the measured output torque to the theoretical average value is increased from 74% to 89% by the reduction of friction on the meshing teeth by

Clear periodical variation is not observed on the measured output torque wave. It is considered that the friction inside the motor disturbs the smooth motion and the presence of the teeth is also one of the causes.

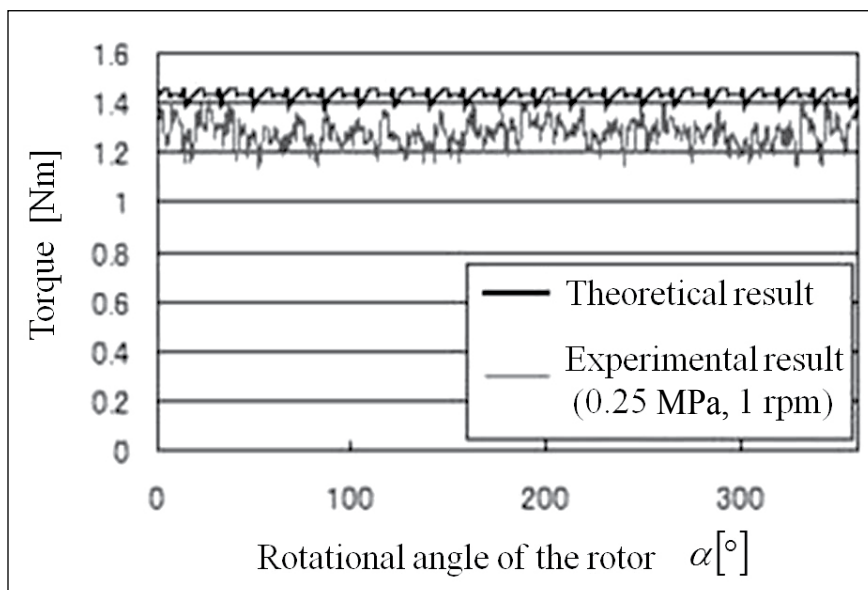


Figure 10. Comparison of calculated and measured output torque (at $P_s=0.25$ MPa)

The theoretical calculation carried out in this paper is based on the contact wheel model in which the presence of the teeth is ignored.

6 Conclusions

The structure and the working principle of LPW-PGM, which can be driven by low pressure as same as civil tap water pressure, is introduced. The mechanism of generation of the output torque is explained clearly and the method of calculation of the theoretical output torque is revealed based on the contact wheel model. It is confirmed that the calculation gives the appropriate result by comparison with the average value of the theoretical torque calculated by another method. The mechanism of generation of the periodical variation in the output torque is also explained based on the theoretical considerations.

The measurement of the output torque with a prototype of the LPW-PGM is carried out under the condi-

tion of very low constant rotational speeds. As a result with the original prototype, the ratio of the average value of the measured output torque to the theoretical average value is 0.74. The surfaces of the planetary gears are put a treatment with solid lubricant film which contains Graphite in order to reduce the friction on the meshing teeth. It increased the ratio of the average value of the measured output torque to the theoretical average value to 0.89. The output torque efficiency increased in about 15% by the surface treatment of the planetary gears. The planetary gear made of PEEK gives also pretty good improvement in the output torque. It is found that the friction on the meshing teeth has considerably a large effect on the output torque efficiency.

As a result of the comparison of the theoretical and experimental results, it is found that there is still the difference of 0.15 Nm between the average values of them even with the surface treatment on the plan-

etary gears. The more reduction of torque loss is expected to improve moreover the output torque of LPW-PGM.

References

- [1] Modern Water Hydraulics – Your Choice for the Future. Booklet of Introduction of Water Hydraulics published by NFPA, 1995, pp.1-5.
- [2] Aaltonen J. & Koskinen K. T. & Vilenius M. & Kunttu P. 1999. Experiences On The Low Pressure Water Hydraulic Systems, Proceedings of the Fourth JFPS International Symposium, November 15-17, Tokyo, Japan, pp.357-363.
- [3] Kunttu P. & Koskinen K. T. & Vilenius M. 1999. Low Pressure Water Hydraulics -State of the Art, Proceedings of The Sixth Scandinavian International Conference on Fluid Power, May 26–28, Tampere, Finland, pp.67-75.
- [4] Aqua Drive System – A Technical Guide 2. Booklet of Introduction of Water Hydraulics published by JFPA, 2005, pp.36-39.
- [5] J.W.G.M. Huijbers. 1990. Kinematics of the Planetary Gear Motor, Report PGM-T1, Hessels & van Rooij Engineering.
- [6] Oshima S. & Suzuki T. & Oobayashi Y. & Miyakawa S. 2006. Development of a Low Pressure Water Hydraulic Planetary Gear Motor, Proceedings of JSME Annual Conference 2006 (in Japanese), September 18-22, Kumamoto, Japan, Vol.2, pp.327-328.
- [7] Mizutani J. & Nishida T. & Mutoh Y. & Kawamura M. & Imaoka R. & Satoh M. 2008. Effect of Solid Lubricant Film on Fretting Fatigue Strength of Aluminum Alloy (JIS A7N01), Transaction of the Japan Society of Mechanical Engineers (in Japanese), Vol.74 No.744, pp.1126-1133.

**dnevi
slovenske
informatike**

“Ustvarimo nove rešitve!”

Kongresni center Grand hotel Bernardin Portorož
Slovenija | 16. - 18. april 2012 | www.dsl2012.si

Nomenclature

F_{G1}, F_{G2}	tangential forces on the surface of the rotor, which are generated by pressure acts on the planetary gears
F_r	radial force on the rotor, which is generated by pressure acts on the rotor
f_1, f_2	forces generated by pressure acts on the planetary gears
l_1	distance between the contact points of the next two planetary gears' pitch circles and the pitch curve of the rotor
l_2	distance from the center of the rotor to the force acting line of F_r
N_{rRL}	number of lobes on the rotor
N_{rSL}	number of lobes on the stator
P_c	pressure in the displacement chamber
P_S	supply pressure
R_{r0}	minimum radius of the rotor's pitch curve
R_r^m	maximum radius of the rotor's pitch curve
R_{s0}	minimum radius of the stator's pitch curve
R_s^m	maximum radius of the stator's pitch curve
R_p	radius of the planetary gear's pitch circle
$r_R(\theta)$	radius of the rotor's pitch curve at a given tangential position θ
r_1, r_2	distance from the center of the rotor (and also stator) to the contact points of the planetary gears' pitch circles and the pitch curve of the rotor
s_1, s_2	distance from the center of the rotor (and also stator) to the contact points of the planetary gears' pitch circles and the pitch curve of the stator
T^{th}	theoretical output torque
T_G	torque generated by pressure act on the planetary gears
T_r	torque generated by pressure act on the rotor
V^{th}	theoretical displacement volume
W_P	width of the rotor, stator and planetary gears
α	rotational angle of the rotor's rotation
θ	tangential position angle on the coordinate systems defined on the rotor (see Fig. 3)
θ_1, θ_2	tangential position angles of the contact points of the planetary gears' pitch circles and the pitch curves of the stator and rotor, which are given on the coordinate systems defined on the stator (see Fig. 4)

Raziskave izhodnega momenta nizekotlačnega vodnohidravličnega planetnega zobniškega motorja

Razširjeni povzetek

Prispevek obravnava nizekotlačni planetni zobniški hidravlični motor, ki deluje na vodo iz pipe. Nizekotlačna vodna hidravlika ima prednosti, kot so nizka cena, varnost, enostavna uporaba in predvsem prijaznost do naravnega okolja – ni tveganja zaradi onesnaževanja, ko se pojavi zunanje puščanje hidravlične kapljevine. Namen prispevka je prikazati konstrukcijo nizekotlačnega vodnega hidravličnega planetnega zobniškega motorja (LPW-PGM) in razložiti verjeten mehanizem generiranja izhodnega pogonskega momenta motorja ter izračun teoretičnega izhodnega momenta.

Glavni sestavni deli vodnega hidravličnega motorja (LPW-PGM) so (slika 1): stator, rotor, devet planetnih zobnikov, ventilska plošča A in B, sredinska plošča ter prirobnica. Predstavljeni prototip LPW-PGM ima stator s petimi krivuljami in rotor s štirimi. Na krivuljnih površinah statorja in rotorja so izdelani zobje, katerih oblikovni parametri so enaki kot na vmesnih devetih planetnih zobnikih. Geometrija LPW-PGM definira devet komor, ki jih določa rotor, stator, devet vmesnih planetnih zobnikov, ventilska plošča B in prirobnica. Volumen posamične komore se periodično spreminja med vrtenjem rotorja. Iztisnina predstavljenega vodnega hidravličnega motorja je 36,6 cm³/vrt., izhodni moment je 0,75 Nm pri 200 vrt./min in tlaku 2,5 bar.

Moment zobniškega planetnega hidravličnega motorja je sestavljen iz dveh delov (sl. 4). Prvi del momenta nastane pri delovanju tlaka na površino rotorja v posamezni komori. Pogoj za nastanek prvega dela momenta

je ekscentrični položaj te ploskve glede na os vrtenja rotorja (slika 4. a). Drugi del momenta pa nastopi pri delovanju tlaka vode na planetna zobnika posamezne komore (slika 4. b). Rezultanta momentov obeh planetnih zobnikov v posamezni komori deluje v smeri, kjer je planetni zobnik bolj oddaljen od središča vrtenja rotorja. V primeru na sliki 4 se rotor vrti v smeri urnega kazalca.

Teoretično izračunan izhodni moment je primerjan z izmerjenim pri zelo nizkih vrtljajih gredi hidravličnega motorja. Ugotovljena je razlika med izračunanimi in izmerjenimi vrednostmi. Glavni razlog odstopanj je v trenju med statorjem, rotorjem in planetnimi zobniki. Povprečni mehansko-hidravlični izkoristek osnovnega prototipa vodnega hidravličnega motorja je bil 74 %. Eksperimentalni rezultati prikazujejo, da površinska obdelava planetnih zobnikov s trdim mazalnim filmom, ki vsebuje grafit, poveča izhodni moment hidravličnega motorja za 15 %. V nadaljevanju so bili testirani tudi planetni zobniki, izdelani iz polimera poli-eter-eter-ketona (PEEK) in medenine.

Ključne besede: vodna hidravlika, nizek tlak, planetni zobniški motor, izhodni moment

Acknowledgements

This work has been supported by Dr. Shimpei Miyakawa and Yoshihiro Oobayashi of KYB Corporation, Basic Technology R&D Center, Water Hydraulic System Group. The authors would like to thank them for their support with production of the prototype of LPW-PGM.

ISKRA **ame**.si

Naboj za razvoj

Razvoj in proizvodnja naprav za preskušanje:

- števecv električne energije
- merilnih in zaščitnih tokovnih transformatorjev
- merilnih in krmilnih tokovnih pretvornikov
- stikal, varovalk, odklopnikov, motorjev

Razvoj in proizvodnja strojev in naprav za industrijsko avtomatizacijo

Proizvodne storitve na CNC strojih

ISKRA AMESI, d. o. o.
Savska loka 4
SI-4000 Kranj
Slovenia

Tel.: +386 4 206 42 65
Fax.: +386 4 202 26 11
E-mail: info@iskra-ame.si

robosapiens

www.iskra-ame.si